

New Cardinality Estimation Methods for HyperLogLog Sketches

Otmar Ertl
Linz, Austria
otmar.ertl@gmail.com

ABSTRACT

This work presents new cardinality estimation methods for data sets recorded by HyperLogLog sketches. A simple derivation of the original estimator was found, that also gives insight how to correct its deficiencies. The result is an improved estimator that is unbiased over the full cardinality range, is easy computable, and does not rely on empirically determined data as previous approaches. Based on the maximum likelihood principle a second unbiased estimation method is presented which can also be extended to estimate cardinalities of union, intersection, or relative complements of two sets that are both represented as HyperLogLog sketches. Experimental results show that this approach is more precise than the conventional technique using the inclusion-exclusion principle.

1 INTRODUCTION

Counting the number of distinct elements in a data stream or large datasets is a common problem in big data processing. In principle, finding the number of distinct elements n with a maximum relative error ε in a data stream requires $O(n)$ space [1]. However, probabilistic algorithms that achieve the requested precision only with high probability are able to drastically reduce space requirements. Many different probabilistic algorithms have been developed over the past two decades [18, 23] until a theoretically optimal algorithm was finally found [14]. Although this algorithm achieves the optimal space complexity of $O(\varepsilon^{-2} + \log n)$ [1, 13], it is not very efficient in practice [23].

More practicable and already widely used in many applications is the HyperLogLog (HLL) algorithm [11] with a near-optimal space complexity $O(\varepsilon^{-2} \log \log n + \log n)$. A big advantage of the HLL algorithm is that corresponding sketches can be easily merged, which is a requirement for distributed environments. Unfortunately, the originally proposed estimation method has some problems to guarantee the same accuracy over the full cardinality range. Therefore, a couple of variants have been developed to correct the original estimate by empirical means [12, 21, 22].

An estimator for HLL sketches, that does not rely on empirical data and that significantly improves the estimation error, is the historic inverse probability estimator [5, 23]. It trades memory efficiency for mergeability. The estimator needs to be continuously updated while inserting elements and the estimate depends on the insertion order. Moreover, the estimator cannot be further used after merging two sketches, which limits its application to single data streams. If this restriction is acceptable, the self-learning bitmap [4], which provides a similar trade-off and also needs less space than the original HLL method, could be used alternatively.

Sometimes not only the number of distinct elements but also a sample of them is needed in order to allow later filtering according to some predicate and estimating the cardinalities of corresponding subsets. In this case the k-minimum values algorithm [2, 6] is the

Algorithm 1 Insertion of a data element D into a HLL sketch. All registers $K = (K_1, \dots, K_m)$ start from zero.

```

procedure INSERTELEMENT( $D$ )
   $\langle a_1, \dots, a_p, b_1, \dots, b_q \rangle_2 \leftarrow (p+q)$ -bit hash value of  $D$ 
   $i \leftarrow 1 + \langle a_1, \dots, a_p \rangle_2$ 
   $k \leftarrow \min(\{s \mid b_s = 1\} \cup \{q+1\})$ 
  if  $k > K_i$  then
     $K_i \leftarrow k$ 
  end if
end procedure

```

method of choice. It needs more space than the HLL algorithm, but also allows set manipulations like construction of intersections, relative complements, or unions [8]. The latter operation is the only one that is natively supported by HLL sketches. A sketch that represents the set operation result is not always needed. One approach to estimate the corresponding result cardinality directly is based on the inclusion-exclusion principle, which however can lead to large errors, especially if the result is small compared to the input set sizes [8]. Therefore, it was proposed to combine HLL sketches with minwise hashing [7, 19], which improves the estimation error, even though at the expense of significant more space consumption. It was recently pointed out without special focus on HLL sketches, that the application of the maximum likelihood (ML) method to the joint likelihood function of two probabilistic data structures leads to better cardinality estimates for intersections [24].

2 HYPERLOGLOG DATA STRUCTURE

The HLL algorithm collects information of incoming elements into a very compact sketching data structure, that finally allows to estimate the number of distinct elements. The data structure consists of $m = 2^p$ registers. All registers start with zero initial value. The insertion of a data element into a HLL data structure requires the calculation of a $(p+q)$ -bit hash value. The leading p bits of the hash value are used to select one of the 2^p registers. Among the next following q bits, the position of the first 1-bit is determined which is a value in the range $[1, q+1]$. The value $q+1$ is used, if all q bits are zeros. If the position of the first 1-bit exceeds the current value of the selected register, the register value is replaced. The complete update procedure is shown in Algorithm 1.

A HLL sketch can be characterized by the parameter pair (p, q) where the precision parameter p controls the relative estimation error which scales like $1/\sqrt{m}$ [11] while q defines the possible range for registers which is $\{0, 1, \dots, q+1\}$. The case $q = 0$ corresponds to a bit array and shows that the HLL algorithm can be regarded as generalization of linear counting [26]. The number of consumed hash value bits $p+q$ defines the maximum cardinality that can be tracked. Obviously, if the cardinality reaches values in the order of

2^{p+q} , hash collisions will become more apparent and the estimation error will increase.

Algorithm 1 has some properties which are especially useful for distributed data streams. First, the insertion order of elements has no influence on the final sketch state. Furthermore, any two HLL sketches with same parameters (p, q) representing two different sets can be easily merged. The sketch that represents the union of both sets can be constructed by taking the register-wise maximum values.

The state of a HLL sketch is described by the vector $\mathbf{K} = (K_1, \dots, K_m)$. Under the assumption of a uniform hash function the inserted elements are distributed over all m registers according to a multinomial distribution with equal probabilities $1/m$ [11]. Therefore, any permutation of \mathbf{K} is equally likely for a given cardinality. Thus, the order of register values K_1, \dots, K_m contains no information about the cardinality which makes the multiset $\{K_1, \dots, K_m\}$ a sufficient statistic for n . Since the values of the multiset are all in the range $[0, q+1]$, the multiset can also be written as $\{K_1, \dots, K_m\} = 0^{C_0} 1^{C_1} \dots q^{C_q} (q+1)^{C_{q+1}}$ where C_k is the multiplicity of value k . As a consequence, the multiplicity vector $\mathbf{C} := (C_0, \dots, C_{q+1})$, which corresponds to the register value histogram, is also a sufficient statistic for the cardinality. By definition we have $\sum_{k=0}^{q+1} C_k = m$.

2.1 Poisson Approximation

The multinomial distribution is the reason that register values are statistically dependent and that further analysis is difficult. For simplification a Poisson model can be used [11], which assumes that the cardinality itself is distributed according to a Poisson distribution $n \sim \text{Poisson}(\lambda)$. Under the Poisson model the register values are independent and identically distributed according to

$$P(K \leq k | \lambda) = \begin{cases} 0 & k < 0 \\ e^{-\frac{\lambda}{m2^k}} & 0 \leq k \leq q \\ 1 & k > q. \end{cases} \quad (1)$$

The Poisson approximation makes it easier to find an estimator $\hat{\lambda} = \hat{\lambda}(\mathbf{K})$ for the Poisson rate λ than for the cardinality n under the fixed-size model. Depoissonization finally allows to translate the estimates back to the fixed-size model. Assume we have found an estimator $\hat{\lambda}$ for the Poisson rate that is unbiased $\mathbb{E}(\hat{\lambda} | \lambda) = \lambda$ for all $\lambda \geq 0$. This implies $\mathbb{E}(\hat{\lambda} | n) = n$ as it is the only solution of

$$\mathbb{E}(\hat{\lambda} | \lambda) = \sum_{n=0}^{\infty} \mathbb{E}(\hat{\lambda} | n) e^{-\lambda} \frac{\lambda^n}{n!} = \lambda \quad \text{for all } \lambda \geq 0.$$

Hence, the unbiased estimator $\hat{\lambda}$ conditioned on n is also an unbiased estimator for n , which motivates us to use $\hat{\lambda}$ directly as estimator for the cardinality $\hat{n} := \hat{\lambda}$. As our results will show later, this Poisson approximation works well over the full cardinality range, even for estimators that are not exactly unbiased.

3 ORIGINAL ESTIMATION APPROACH

The original cardinality estimator [11] is based on the idea that the number of distinct element insertions a register needs to reach the value k is proportional to $m2^k$. Given that, a rough cardinality estimate can be obtained by averaging the values $\{m2^{K_1}, \dots, m2^{K_m}\}$.

The harmonic mean was found to work best as it is less sensitive to outliers. The result is the so-called raw estimator given by

$$\hat{n}_{\text{raw}} = \alpha_m \frac{m}{\frac{1}{m2^{K_1}} + \dots + \frac{1}{m2^{K_m}}} = \frac{\alpha_m m^2}{\sum_{k=0}^{q+1} C_k 2^{-k}}. \quad (2)$$

Here α_m is a bias correction factor [11] which can be well approximated by $\alpha_{\infty} := \lim_{m \rightarrow \infty} \alpha_m = \frac{1}{2 \log 2}$ in practice, because the additional bias is negligible compared to the overall estimation error.

To investigate the estimation error of the raw estimator and other estimation approaches discussed in the following, we filled 10 000 HLL sketches with up to 50 billion unique elements. To speed up computation we assumed a uniform hash function whose values can be simulated by random numbers. We used the Mersenne Twister random number generator with a state size of 19 937 bits from the C++ standard library.

Fig. 1 shows the distribution of the relative error of the raw estimator as function of the true cardinality for $p = 12$ and $q = 20$. Corrections for small and large cardinalities have been proposed to reduce the obvious bias. For small cardinalities the HLL sketch can be interpreted as bit array by distinguishing between registers with zero and nonzero values. This allows using the linear counting cardinality estimator [26]

$$\hat{n}_{\text{small}} = m \log(m/C_0). \quad (3)$$

The corresponding estimation error is small for small cardinalities and is shown in Fig. 2. It was proposed to use this estimator as long as $\hat{n}_{\text{raw}} \leq \frac{5}{2}m$ where the factor $\frac{5}{2}$ was empirically determined [11]. For large cardinalities in the order of 2^{p+q} , for which a lot of registers are already in a saturated state, meaning that they have reached the maximum possible value $q+1$, the raw estimator underestimates cardinalities. For the 32-bit hash value case ($p+q = 32$), which was considered in [11], following correction formula was proposed if $\hat{n}_{\text{raw}} > 2^{32}/30 \approx 1.43 \times 10^8$ to take these saturated registers into account

$$\hat{n}_{\text{large}} = -2^{32} \log(1 - \hat{n}_{\text{raw}}/2^{32}). \quad (4)$$

The relative estimation error of the original method that includes both corrections is shown in Fig. 3 for the case $p = 12$ and $q = 20$. Unfortunately, the ranges where the estimation error is small for \hat{n}_{raw} and \hat{n}_{small} do not overlap, which causes the estimation error to be much larger near the transition region. To reduce the error for cardinalities close to this region, it was proposed to correct the bias of \hat{n}_{raw} . Empirically collected bias correction data can be either stored as set of interpolation points [12], as lookup table [21], or as best-fitting polynomial [22]. However, all these empirical approaches treat the symptom and not the cause.

The large range correction formula (4) is not satisfying either as it does not reduce the estimation error but makes it even worse. Instead of underestimating cardinalities, they are now overestimated. Another indication for the incorrectness of the proposed large range correction is the fact that it is not even defined for all possible states. For instance, consider a (p, q) -HLL sketch with $p+q = 32$ for which all registers are equal to the maximum possible value $q+1$. The raw estimate would be $\hat{n}_{\text{raw}} = \alpha_m 2^{33}$, which is greater than 2^{32} and outside of the domain of the large range correction formula. A simple approach to avoid the need of any

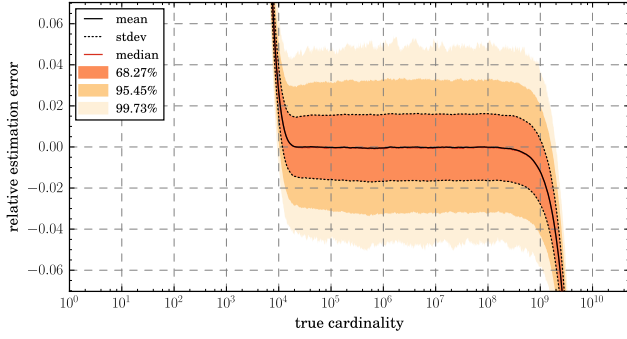


Figure 1: Relative error of the raw estimator for $p = 12$ and $q = 20$.

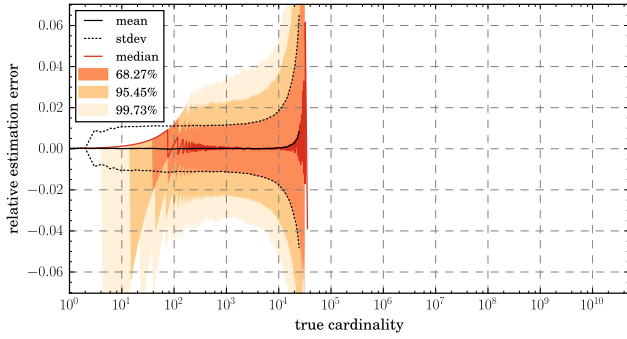


Figure 2: Relative error of the linear counting estimator for bitmap size 4096 which corresponds to $p = 12$ and $q = 0$.

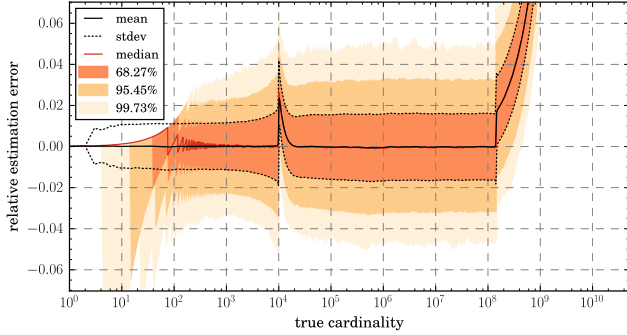


Figure 3: Relative estimation error of the original method for $p = 12$ and $q = 20$.

large range corrections is to extend the operating range of the raw estimator to larger cardinalities. This can be easily accomplished by increasing $p + q$, which corresponds to using hash values with more bits. Each additional bit doubles the operating range which scales like 2^{p+q} . However, in case $q \geq 31$ the number of possible register values, which are $\{0, 1, \dots, q + 1\}$, exceeds 32 and is no longer representable by 5 bits. Therefore, it was proposed to use 6 bits per register in combination with 64-bit hash values [12]. Even

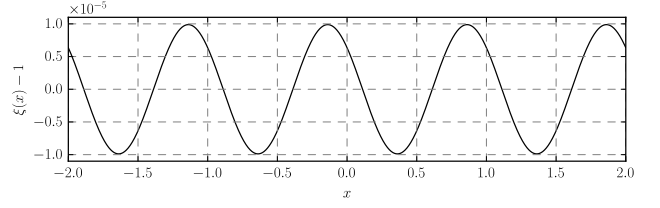


Figure 4: The deviation of $\xi(x)$ from 1.

larger hash values are needless in practice, because it is unrealistic to encounter cardinalities of order 2^{64} .

3.1 Derivation of the Raw Estimator

To better understand why the raw estimator fails for small and large cardinalities, we start with a brief and simple derivation without the restriction to large cardinalities ($n \rightarrow \infty$) and without using complex analysis as in [11]. Assume that the register values have following cumulative distribution function

$$P(K \leq k | \lambda) = e^{-\frac{\lambda}{m2^k}}. \quad (5)$$

For now we ignore that this distribution has infinite support and differs from the register value distribution under the Poisson model (1), whose support is limited to $[0, q + 1]$. For a random variable K obeying (5) the expectation of 2^{-K} is given by

$$\mathbb{E}(2^{-K}) = \frac{1}{2} \sum_{k=-\infty}^{\infty} 2^{-k} e^{-\frac{\lambda}{m2^k}} = \frac{\alpha_{\infty} m \xi(\log_2(\lambda/m))}{\lambda}, \quad (6)$$

where the function

$$\xi(x) := \log(2) \sum_{k=-\infty}^{\infty} 2^{k+x} e^{-2^{k+x}}$$

is a smooth periodic oscillating function with mean 1 and an amplitude that can be bounded by $\eta := 9.885 \times 10^{-6}$ as shown in Fig. 4. This limit can also be found using Fourier analysis [10]. For a large ($m \rightarrow \infty$) sample K_1, \dots, K_m , that is distributed according to (5), we asymptotically have

$$\mathbb{E}\left(\frac{1}{2^{-K_1} + \dots + 2^{-K_m}}\right) \stackrel{m \rightarrow \infty}{=} \frac{1}{\mathbb{E}(2^{-K_1} + \dots + 2^{-K_m})} = \frac{1}{m \mathbb{E}(2^{-K})}.$$

Together with (6) we obtain

$$\lambda = \mathbb{E}\left(\frac{\alpha_{\infty} m^2 \xi(\log_2(\lambda/m))}{2^{-K_1} + \dots + 2^{-K_m}}\right) \quad \text{for } m \rightarrow \infty.$$

Therefore, the asymptotic relative bias of

$$\hat{\lambda} = \frac{\alpha_{\infty} m^2}{2^{-K_1} + \dots + 2^{-K_m}}$$

is bounded by η , which makes this statistic a good estimator for the Poisson parameter. It also corresponds to the raw estimator (2), if the Poisson parameter estimate is used as cardinality estimate as discussed in Section 2.1.

3.2 Limitations of the Raw Estimator

The raw estimator is based on two prerequisites. In practice, only the first requiring m to be sufficiently large is satisfied. However, the second assuming that the distribution of register values (1) can be approximated by (5) is not always true. A random variable K' with cumulative distribution function (5) can be transformed into a random variable K with cumulative distribution function (1) using

$$K = \min(\max(K', 0), q + 1). \quad (7)$$

Therefore, register values K_1, \dots, K_m can be seen as the result after applying this transformation to a sample K'_1, \dots, K'_m from (5). If all registers values are in the range $[1, q]$, they must be identical to the values K'_1, \dots, K'_m . In other words, the observed register values are also a plausible sample of distribution (5). Hence, as long as all or at least most register values are in the range $[1, q]$, which is the case if $2^p \ll \lambda \ll 2^{p+q}$, the approximation of (1) by (5) is valid. This explains why the raw estimator works best for intermediate cardinalities. However, for small and large cardinalities many register values are equal to 0 or $q + 1$, respectively, which contradicts (5) and ends up in the observed bias.

4 IMPROVED ESTIMATOR

If we knew the values K'_1, \dots, K'_m for which transformation (7) led to the observed register values K_1, \dots, K_m , we would be able to use the raw estimator

$$\hat{\lambda} = \frac{\alpha_\infty m^2}{\sum_{k=-\infty}^{\infty} C'_k 2^{-k}} \quad (8)$$

where $C'_k := |\{i | k = K'_i\}|$ are the multiplicities of value k in $\{K'_1, \dots, K'_m\}$. Due to (7), the multiplicities C'_k and the multiplicities C_k for the observed register values have following relationships

$$C_0 = \sum_{k=-\infty}^0 C'_k, \quad C_k = C'_k \quad (1 \leq k \leq q), \quad C_{q+1} = \sum_{k=q+1}^{\infty} C'_k. \quad (9)$$

The idea is now to find estimates \hat{c}'_k for all $k \in \mathbb{Z}$ and use them as replacements for C'_k in (8). For $k \in [1, q]$ we can use the trivial estimators $\hat{c}'_k := C_k$. Estimators for $k \leq 0$ and $k \geq q + 1$ can be found by considering the expectation of C'_k

$$\mathbb{E}(C'_k) = m P(K' = k | \lambda) = m e^{-\frac{\lambda}{m 2^k}} \left(1 - e^{-\frac{\lambda}{m 2^k}}\right).$$

According to (1) we have $\mathbb{E}(C_0/m) = e^{-\frac{\lambda}{m}}$ and $\mathbb{E}(1 - C_{q+1}/m) = e^{-\frac{\lambda}{m 2^q}}$ which gives

$$\begin{aligned} \mathbb{E}(C'_k) &= m (\mathbb{E}(C_0/m))^{2^{-k}} \left(1 - (\mathbb{E}(C_0/m))^{2^{-k}}\right), \\ &= m (\mathbb{E}(1 - C_{q+1}/m))^{2^{q-k}} \left(1 - (\mathbb{E}(1 - C_{q+1}/m))^{2^{q-k}}\right). \end{aligned}$$

These two expressions for the expectation suggest to use

$$\begin{aligned} \hat{c}'_k &= m (C_0/m)^{2^{-k}} \left(1 - (C_0/m)^{2^{-k}}\right) \quad \text{and} \\ \hat{c}'_k &= m (1 - C_{q+1}/m)^{2^{q-k}} \left(1 - (1 - C_{q+1}/m)^{2^{q-k}}\right) \end{aligned}$$

as estimators for $k \leq 0$ and $k \geq q + 1$, respectively. Both estimators conserve the mass of zero-valued and saturated registers, because

(9) is satisfied, if C'_k is replaced by \hat{c}'_k . Plugging all these estimators into (8) as replacements for C'_k finally gives

$$\hat{\lambda} = \frac{\alpha_\infty m^2}{m \sigma(C_0/m) + \sum_{k=1}^q C_k 2^{-k} + m \tau(1 - C_{q+1}/m) 2^{-q}} \quad (10)$$

which we call the improved estimator. Here $m \sigma(C_0/m)$ and $m \tau(1 - C_{q+1}/m)$ are replacements for C_0 and C_{q+1} in the raw estimator (2), respectively. The functions σ and τ are defined as

$$\sigma(x) := x + \sum_{k=1}^{\infty} x^{2^k} 2^{k-1}, \quad (11)$$

$$\tau(x) := \frac{1}{3} \left(1 - x - \sum_{k=1}^{\infty} (1 - x^{2^{-k}})^2 2^{-k}\right). \quad (12)$$

We can cross-check the new estimator for the linear counting case with $q = 0$. Using the identity

$$\sigma(x) + \tau(x) = \alpha_\infty \xi(\log_2(\log(1/x))) / \log(1/x), \quad (13)$$

we get

$$\hat{\lambda} = \frac{\alpha_\infty m}{\sigma(C_0/m) + \tau(C_0/m)} = \frac{m \log(m/C_0)}{\xi(\log_2(\log(m/C_0)))}$$

which is as expected almost identical to the linear counting estimator (3), because $\xi(x) \approx 1$.

The new estimator can be directly translated into an estimation algorithm that does not depend on magic numbers or special cases as previous approaches. Since $C_k \in \{0, \dots, m\}$, the values for $m \sigma(C_0/m)$ and $m \tau(1 - C_{q+1}/m)$ can be precalculated and kept in lookup tables of size $m + 1$. In this way a complete branch-free cardinality estimation can be realized. However, on-demand calculation of σ and τ is very fast as well. The series (11) converges quadratically for all $x \in [0, 1)$ and its terms can be calculated recursively using elementary operations. The case $x = 1$ needs special handling, because the series diverges and causes an infinite denominator in (10) and therefore a vanishing cardinality estimate. As this case only occurs if all register values are in initial state ($C_0 = m$), this is exactly what is expected. Apart from the trivial roots at $x = 0$ and $x = 1$, the calculation of τ is slightly more expensive, because it involves square root evaluations and its series converges only linearly. Since $1 - x^{2^{-k}} \leq -\log(x) 2^{-k}$ for $x \in (0, 1]$ its convergence speed is comparable to a geometric series with ratio $1/8$. It is also thinkable to calculate τ using the approximation $\tau(x) \approx \alpha_\infty / \log(1/x) - \sigma(x)$ which can be obtained from (13) and $\xi(x) \approx 1$. The advantage is that the calculation of σ and the additional logarithm is slightly faster than the direct calculation of τ using (12). However, for arguments close to 1 both terms may become very large compared to their difference, which requires special care to avoid numerical cancellation. The calculation of τ can be omitted at all, if the HLL parameters are chosen such that 2^{p+q} is much larger than the expected cardinality. The number of saturated registers is negligible in this case ($C_{q+1} \approx 0$) and therefore $\tau(1 - C_{q+1}/m) \approx \tau(1) = 0$.

4.1 Results

Fig. 5 shows the relative estimation error of the new improved estimator, again based on 10 000 randomly generated HLL sketches with parameters $p = 12$ and $q = 20$. The experimental results

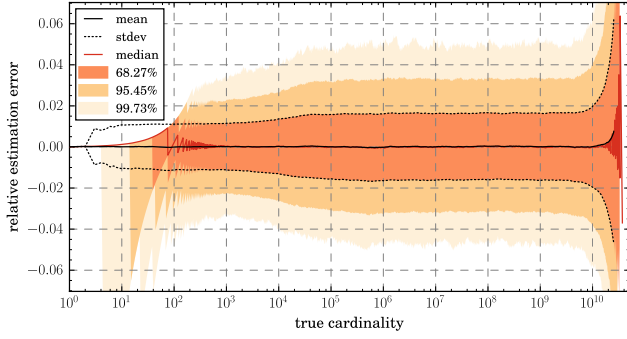


Figure 5: Relative error of the improved estimator for $p = 12$ and $q = 20$.

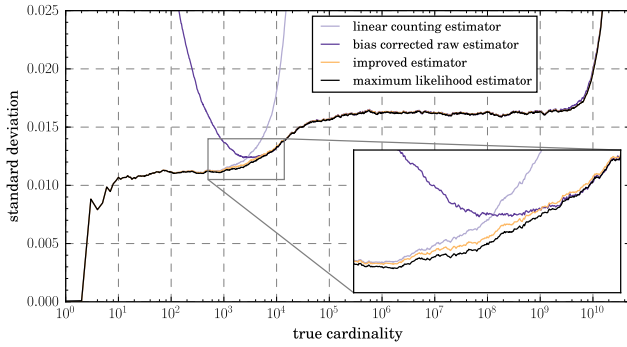


Figure 6: Standard deviations of the relative error of different cardinality estimators for $p = 12$ and $q = 20$.

show that new estimator is unbiased up to cardinalities of 10 billions which is a clear improvement over the raw estimator (compare Fig. 1). The improved estimator beats the precision of existing methods that apply bias correction on the raw estimator (2) [12, 21, 22]. Based on the simulated data we have empirically determined the bias correction function w_{corr} that satisfies $n = \mathbb{E}(w_{\text{corr}}(\hat{n}_{\text{raw}})|n)$ for all cardinalities. By definition, the estimator $\hat{n}'_{\text{raw}} := w_{\text{corr}}(\hat{n}_{\text{raw}})$ is unbiased and a function of the raw estimator. Its standard deviation is compared with that of the improved estimator in Fig. 6. For cardinalities smaller than 10^4 the empirical bias correction approach had to switch over to the linear counting estimator at some point. The standard deviation of the linear counting estimator is also shown in Fig. 6. Obviously, the previous approaches cannot do better than given by the minimum of both curves for linear counting and raw estimator. In practice, the standard deviation of the combined approach is even larger, because the choice between both estimators must be made based on an estimate and not on the true cardinality, for which the intersection point of both curves, which is approximately 3×10^3 in Fig. 6, would be the ideal transition point. In contrast, the improved estimator performs well over the entire cardinality range.

We also investigated the estimation error of the improved estimator for the case $p = 22, q = 10$ as shown in Fig. 7. The standard

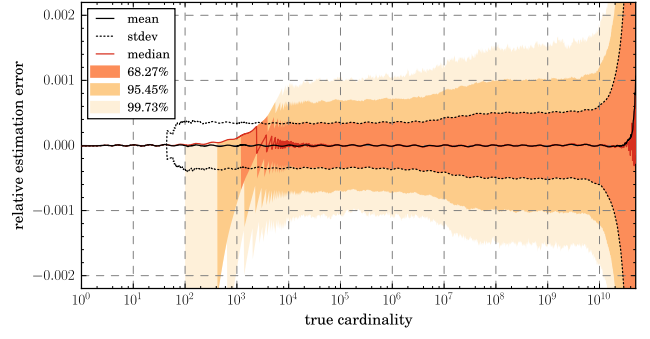


Figure 7: Relative error of the improved estimator for $p = 22$ and $q = 10$.

deviation is by a factor 32 smaller according to the $1/\sqrt{m}$ error scaling law. Again, cardinalities up to order $2^{p+q} \approx 4 \times 10^9$ can be well estimated, because $p + q = 32$ was kept the same for both investigated HLL configurations. For $p = 22$ a small oscillating bias becomes apparent, which is caused by approximating the periodic function ξ by a constant (see Section 3.1).

5 MAXIMUM LIKELIHOOD ESTIMATION

We know from Section 2.1 that any unbiased estimator for the Poisson parameter is also an unbiased estimator for the cardinality. Moreover, we know that under suitable regularity conditions of the probability mass function the ML estimator is asymptotically efficient [3]. This means, if the number of registers m is sufficiently large, the estimator should be unbiased.

The log-likelihood function for given register values \mathbf{K} , which are assumed to be distributed according to (1) under the Poisson model, is

$$\log \mathcal{L}(\lambda|\mathbf{K}) = \sum_{k=1}^{q+1} \log \left(1 - e^{-\frac{\lambda}{m 2^{\min(k,q)}}} \right) C_k - \frac{\lambda}{m} \sum_{k=0}^q \frac{C_k}{2^k}. \quad (14)$$

After differentiation and multiplying by λ we find that the ML estimate $\hat{\lambda}$ is the unique root of the monotone decreasing function

$$f(\lambda) = \sum_{k=1}^{q+1} \frac{\frac{\lambda}{m 2^{\min(k,q)}}}{e^{\frac{\lambda}{m 2^{\min(k,q)}}} - 1} C_k - \frac{\lambda}{m} \sum_{k=0}^q \frac{C_k}{2^k}.$$

Since $f(0) = m - C_0 \geq 0$ and f is at least linear decreasing as long as $C_{q+1} < m$, there exists a unique root. The special case $C_{q+1} = m$, for which all registers have reached the maximum possible value, the ML estimate would be positive infinite.

Using $f(\hat{\lambda}) = 0$ and $1 - \frac{x}{2} \leq \frac{x}{e^x - 1} \leq 1$ we obtain following bounds for $\hat{\lambda}$

$$\frac{m(m - C_0)}{C_0 + \frac{3}{2} \sum_{k=1}^q \frac{C_k}{2^k} + \frac{C_{q+1}}{2^{q+1}}} \leq \hat{\lambda} \leq \frac{m(m - C_0)}{\sum_{k=0}^q \frac{C_k}{2^k}}. \quad (15)$$

If the cardinality is in the intermediate range, where $C_0 = C_{q+1} = 0$ the lower and the upper bound differ only by a constant factor and both are proportional to the harmonic mean of $\{m 2^{K_1}, \dots, m 2^{K_m}\}$. Hence, consequent application of the ML method would have directly suggested to use a cardinality estimator that is proportional

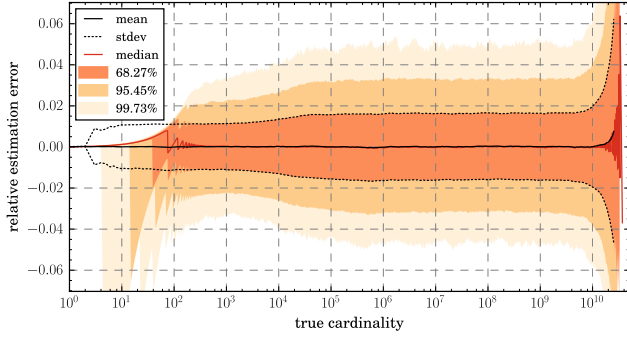


Figure 8: Relative error of the ML estimator for $p = 12$ and $q = 20$.

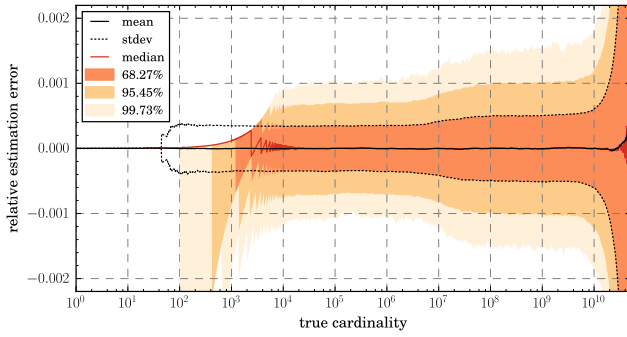


Figure 9: Relative error of the ML estimator for $p = 22$ and $q = 10$.

to the harmonic mean without knowing the raw estimator (2) in advance. The history of the HLL algorithm shows that the raw estimator was first found after several attempts using the geometric mean [9, 11].

For $q = 0$, which corresponds to the linear counting case, the ML estimator can be found by analytical means. The result is exactly the linear counting estimator (3) which makes us optimistic that the ML method in combination with the Poisson model also works well for the more general HLL case $q > 0$. Since f is convex, Newton-Raphson iteration and the secant method [20] will both converge to the root, provided that the function is positive for the chosen starting points. Even though the secant method has the disadvantage of slower convergence, a single iteration is simpler to calculate as it does not require the evaluation of the first derivative. Possible starting points are zero and the lower bound in (15). The iteration can be stopped, if the relative increment is below a certain limit δ . Since the expected estimation error scales according to $1/\sqrt{m}$, it makes sense to choose $\delta = \varepsilon/\sqrt{m}$ with some constant ε . For our results presented below we used $\varepsilon = 10^{-2}$. In practice, only a handful of iterations are necessary to satisfy the stop criterion.

5.1 Results

We have investigated the estimation error of the ML estimator for both HLL configurations as for the improved estimator. Figs. 8

and 9 look very similar to Figs. 5 and 7, respectively. For $p = 12$, $q = 20$ the ML estimator has a somewhat smaller median bias for cardinalities around 200. In addition, the standard deviation of the relative error is marginally better than that of the improved estimator for cardinalities between 10^3 and 10^4 as shown in Fig. 6. For $p = 22$, $p = 10$ we see that the the ML estimator does not have the small oscillating bias as the improved estimator. Since all observed improvements are not very relevant in practice, the improved estimator should be preferred over the ML method, because it leads to a simpler and faster algorithm.

6 JOINT ESTIMATION

While the union of two sets that are represented by HLL sketches can be straightforwardly obtained by taking the register-wise maximums, the computation of cardinalities for other set operations like intersections and relative complements is more challenging. The conventional approach uses the inclusion-exclusion principle

$$\begin{aligned} |S_1 \setminus S_2| &= |S_1 \cup S_2| - |S_2|, & |S_2 \setminus S_1| &= |S_1 \cup S_2| - |S_1|, \\ |S_1 \cap S_2| &= |S_1| + |S_2| - |S_1 \cup S_2|. \end{aligned} \quad (16)$$

It allows to express set operation cardinalities in terms of the union cardinality. However, this approach can lead to very large estimation errors, especially if the result is small compared to the operand cardinalities [8]. In the worst case, the estimate could be negative without artificial restriction to nonnegative values.

Motivated by the good results we have obtained for a single HLL sketch using the ML method in combination with the Poisson approximation, we applied the same approach also for the estimation of set operation result sizes. Assume two given HLL sketches with register values $K_1 = (K_{11}, \dots, K_{1m})$ and $K_2 = (K_{21}, \dots, K_{2m})$ representing sets S_1 and S_2 , respectively. The goal is to find estimates for the cardinalities of the pairwise disjoint sets $A = S_1 \setminus S_2$, $B = S_2 \setminus S_1$, and $X = S_1 \cap S_2$. The Poisson approximation allows us to assume that pairwise distinct elements are inserted into the sketches representing S_1 and S_2 at rates λ_a and λ_b , respectively. Furthermore, we assume that further unique elements are inserted into both sketches simultaneously at rate λ_x . We expect that good estimates $\hat{\lambda}_a$, $\hat{\lambda}_b$, and $\hat{\lambda}_x$ for the rates are also good estimates for the cardinalities $|A|$, $|B|$, and $|X|$.

6.1 Joint Log-Likelihood Function

In order to apply the ML method, we need to find the joint probability distribution of both sketches. Under the Poisson model the individual registers are independent and identically distributed. Therefore, we first derive the joint probability distribution for a single register that has value K_1 in the first sketch that represents S_1 and value K_2 in the second that represents S_2 . The first one can be thought to be constructed by merging two sketches representing A and X , respectively. Analogously, the sketch for S_2 could have been obtained from sketches for B and X . Let K_a , K_b , and K_x be the values of the considered register in the sketches for A , B , and X , respectively. The corresponding values in sketches for S_1 and S_2 are given by $K_1 = \max(K_a, K_x)$ and $K_2 = \max(K_b, K_x)$. Since A , B , and X are disjoint and therefore K_a , K_b , and K_x are independent, the joint cumulative probability function of K_1 and K_2 is

$$P(K_1 \leq k_1 \wedge K_2 \leq k_2) =$$

$$P(K_a \leq k_1) P(K_b \leq k_2) P(K_x \leq \min(k_1, k_2)) = \begin{cases} 0 & k_1 < 0 \vee k_2 < 0 \\ e^{-\frac{\lambda_a}{m^{2k_1}} - \frac{\lambda_b}{m^{2k_2}} - \frac{\lambda_x}{m^{2\min(k_1, k_2)}}} & 0 \leq k_1 \leq q \wedge 0 \leq k_2 \leq q \\ e^{-\frac{\lambda_b + \lambda_x}{m^{2k_2}}} & 0 \leq k_2 \leq q < k_1 \\ e^{-\frac{\lambda_a + \lambda_x}{m^{2k_1}}} & 0 \leq k_1 \leq q < k_2 \\ 1 & q < k_1 \wedge q < k_2. \end{cases} \quad (17)$$

Here we used that K_a , K_b , and K_x follow (1) under the Poisson model. The corresponding probability mass function is

$$\rho(k_1, k_2) = P(K_1 \leq k_1 \wedge K_2 \leq k_2) - P(K_1 \leq k_1 - 1 \wedge K_2 \leq k_2) - P(K_1 \leq k_1 \wedge K_2 \leq k_2 - 1) + P(K_1 \leq k_1 - 1 \wedge K_2 \leq k_2 - 1).$$

Since the values for different registers are independent under the Poisson model, the joint probability mass function for all registers in both sketches is $\rho(\mathbf{k}_1, \mathbf{k}_2) = \prod_{i=1}^m \rho(k_{1i}, k_{2i})$. The ML estimates $\hat{\lambda}_a$, $\hat{\lambda}_b$, and $\hat{\lambda}_x$ can be finally obtained by maximizing the log-likelihood function given by

$$\begin{aligned} \log \mathcal{L}(\lambda_a, \lambda_b, \lambda_x | \mathbf{K}_1, \mathbf{K}_2) &= \sum_{i=1}^m \log(\rho(K_{1i}, K_{2i})) = \\ &= \sum_{k=1}^q \log \left(1 - e^{-\frac{\lambda_a + \lambda_x}{m^{2k}}} \right) C_{1k}^< + \log \left(1 - e^{-\frac{\lambda_b + \lambda_x}{m^{2k}}} \right) C_{2k}^< \\ &+ \sum_{k=1}^{q+1} \log \left(1 - e^{-\frac{\lambda_a}{m^{2\min(k, q)}}} \right) C_{1k}^> + \log \left(1 - e^{-\frac{\lambda_b}{m^{2\min(k, q)}}} \right) C_{2k}^> \\ &+ \sum_{k=1}^{q+1} \log \left(1 - e^{-\frac{\lambda_a + \lambda_x}{m^{2\min(k, q)}}} - e^{-\frac{\lambda_b + \lambda_x}{m^{2\min(k, q)}}} + e^{-\frac{\lambda_a + \lambda_b + \lambda_x}{m^{2\min(k, q)}}} \right) C_k^= \\ &- \frac{\lambda_a}{m} \sum_{k=0}^q \frac{C_{1k}^< + C_k^= + C_{1k}^>}{2^k} - \frac{\lambda_b}{m} \sum_{k=0}^q \frac{C_{2k}^< + C_k^= + C_{2k}^>}{2^k} \\ &- \frac{\lambda_x}{m} \sum_{k=0}^q \frac{C_{1k}^< + C_k^= + C_{2k}^<}{2^k} \end{aligned} \quad (18)$$

where $C_{1k}^<$, $C_{1k}^>$, $C_{2k}^<$, $C_{2k}^>$, and $C_k^=$ are defined as

$$\begin{aligned} C_{1k}^< &:= |\{i | k = K_{1i} < K_{2i}\}|, & C_{1k}^> &:= |\{i | k = K_{1i} > K_{2i}\}|, \\ C_{2k}^< &:= |\{i | k = K_{2i} < K_{1i}\}|, & C_{2k}^> &:= |\{i | k = K_{2i} > K_{1i}\}|, \\ C_k^= &:= |\{i | k = K_{1i} = K_{2i}\}| \end{aligned} \quad (19)$$

for $0 \leq k \leq q+1$. These $5(q+2)$ values represent a sufficient statistic for estimating λ_a , λ_b , and λ_x and greatly reduce the number of terms and also the evaluation costs of the log-likelihood function. The derived formula is the generalization of (14) to two sketches and therefore has a similar structure.

6.2 Numerical Optimization

The ML estimates $\hat{\lambda}_a$, $\hat{\lambda}_b$, and $\hat{\lambda}_x$ are obtained by maximizing (18). Since the three parameters are all nonnegative, this is a constrained optimization problem. The transformation $\lambda = e^\vartheta$ helps to get rid of these constraints and also translates relative accuracy limits into absolute ones, because $\Delta\vartheta = \Delta\lambda/\lambda$. Many optimizer implementations allow the definition of absolute limits rather than relative ones.

Quasi-Newton methods are commonly used to find the maximum of such multi-dimensional functions. They all require the computation of the gradient which can be straightforwardly derived for (18). Among these methods the Broyden-Fletcher-Goldfarb-Shanno (BFGS) algorithm [20] is very popular. We used the implementation provided by the Dlib C++ library [15] for our experiments. Good initial guess values are important to ensure fast convergence for any optimization algorithm. An obvious choice are the cardinality estimates obtained by application of the inclusion-exclusion principle (16). However, in order to ensure that their logarithms are all defined, we require that the initial values are not smaller than 1. The optimization loop is continued until the relative changes of λ_a , λ_b , and λ_x are all smaller than a predefined threshold. For the results presented below we used again $\delta = \varepsilon/\sqrt{m}$ with $\varepsilon = 10^{-2}$. A few tens of iterations are typically necessary to satisfy this stop criterion for starting points determined by the inclusion-exclusion principle.

6.3 Results

To evaluate the estimation error of the new joint cardinality estimation approach we have randomly generated 3000 independent pairs of sketches for which the relative complement cardinalities $|A|$ and $|B|$ and the intersection cardinality $|X|$ are known. Each pair is constructed by randomly generating three HLL sketches filled with $|A|$, $|B|$, and $|X|$ distinct elements, respectively. Then we merged the first with the third and the second with the third to get sketches for $S_1 = A \cup X$ and $S_2 = B \cup X$, respectively.

Table 1 shows the results for HLL sketches with parameters $p = 16$ and $q = 16$. For different cardinality configurations $|A|$, $|B|$, and $|X|$ we have compared the conventional approach using the inclusion-exclusion principle with the new joint ML approach. Among the considered cases there are also cardinalities that are small compared to the number of registers in order to prove that the new approach also covers the small cardinality range where many registers are still in initial state. We have determined the relative root-mean-square error (RMSE) from the estimates for $|A| = |S_1 \setminus S_2|$, $|B| = |S_2 \setminus S_1|$, and $|X| = |S_1 \cap S_2|$ for all 3000 generated examples. In addition, we investigated the estimation error of $\hat{\lambda}_a + \hat{\lambda}_b + \hat{\lambda}_x$ for the union cardinality $|U| = |S_1 \cup S_2|$. We also calculated the improvement factor which we defined as the RMSE ratio between both approaches. Since we only observed values greater than one, the new ML estimation approach improves the precision for all investigated cases. For some cases the improvement factor is even clearly greater than two. Due to the square root scaling of the error, this means that we would need four times more registers to get the same error when using the conventional approach. As the results suggest the new method works well over the full cardinality range without the need of special handling of small or large cardinalities. Obviously, the joint estimation algorithm is also able to reduce the estimation error for unions by a significant amount.

A reason why the ML method performs better than the inclusion-exclusion method is that the latter only uses a fraction of the available information given by the sufficient statistic (19), because the corresponding estimator can be expressed as a function of just the three vectors $(C_1^< + C^= + C_1^>)$, $(C_2^< + C^= + C_2^>)$, and $(C_1^> + C^= + C_2^>)$. In

Table 1: The cardinalities of $A = S_1 \setminus S_2$, $B = S_2 \setminus S_1$, $X = S_1 \cap S_2$, and $U = S_1 \cup S_2$ have been estimated from 3000 different HLL sketch pairs with $p = 16$ and $q = 16$ representing randomly generated sets S_1 and S_2 with fixed intersection and relative complement cardinalities. We have determined the RMSE for the inclusion-exclusion principle and the ML approach together with the corresponding improvement factor for 40 different cases.

	true cardinalities			RMSE inclusion-exclusion				RMSE maximum likelihood				RMSE improvement factor			
	A	B	X	A	B	X	U	A	B	X	U	A	B	X	U
1	69 051	43 258	818	4.83E-3	6.77E-3	3.19E-1	3.16E-3	3.35E-3	3.80E-3	1.30E-1	2.30E-3	1.44	1.78	2.45	1.38
2	429 886 036	170 398 425	45 365 204	5.76E-3	1.04E-2	3.59E-2	4.10E-3	4.60E-3	6.63E-3	2.05E-2	3.35E-3	1.25	1.57	1.75	1.22
3	3 808 040	680 932	1530	4.71E-3	1.46E-2	4.49	4.67E-3	4.08E-3	4.90E-3	1.30	3.52E-3	1.15	2.98	3.45	1.33
4	397 877	18 569	48 262	4.36E-3	2.75E-2	1.08E-2	3.76E-3	4.06E-3	1.99E-2	8.13E-3	3.50E-3	1.08	1.38	1.33	1.07
5	239 529	24 778	326	3.97E-3	1.69E-2	1.03	3.81E-3	3.60E-3	6.59E-3	4.46E-1	3.27E-3	1.10	2.56	2.31	1.16
6	165 754	53 843	108	4.57E-3	9.82E-3	3.26	4.37E-3	3.43E-3	3.69E-3	1.10	2.67E-3	1.33	2.66	2.97	1.64
7	1 667 351	3974	142 771	4.36E-3	1.21E-1	4.74E-3	4.02E-3	4.22E-3	9.77E-2	4.30E-3	3.89E-3	1.03	1.24	1.10	1.03
8	69 742	1058	115	3.03E-3	3.69E-2	3.37E-1	2.98E-3	2.98E-3	1.89E-2	1.71E-1	2.93E-3	1.02	1.95	1.96	1.02
9	871 306 344	3 808 040	66 873 869	4.43E-3	8.90E-2	6.51E-3	4.11E-3	4.27E-3	7.28E-2	5.83E-3	3.96E-3	1.04	1.22	1.12	1.04
10	362 986 091	32 023 944	6 781 734	4.49E-3	1.98E-2	9.20E-2	4.07E-3	4.18E-3	1.08E-2	4.72E-2	3.80E-3	1.07	1.84	1.95	1.07
11	9 050 248	342 712	71 854	4.15E-3	3.04E-2	1.44E-1	3.98E-3	4.03E-3	1.48E-2	6.87E-2	3.86E-3	1.03	2.05	2.10	1.03
12	708 580	1038	42 830	4.13E-3	1.48E-1	4.65E-3	3.89E-3	4.04E-3	1.17E-1	4.09E-3	3.81E-3	1.02	1.27	1.14	1.02
13	50 111 408	54 381	38 388	4.11E-3	1.73E-1	2.45E-1	4.11E-3	4.12E-3	1.07E-1	1.52E-1	4.11E-3	1.00	1.61	1.61	1.00
14	647 883	574 964	8380	6.64E-3	7.09E-3	4.08E-1	3.93E-3	4.29E-3	4.35E-3	1.47E-1	2.86E-3	1.55	1.63	2.78	1.37
15	535 085 964	55 907 711	49 124 015	4.80E-3	1.91E-2	2.15E-2	4.10E-3	4.37E-3	1.28E-2	1.42E-2	3.75E-3	1.10	1.49	1.51	1.09
16	6 125 762 237	23 524 057	142 456 034	4.36E-3	1.08E-1	1.83E-2	4.25E-3	4.33E-3	9.79E-2	1.67E-2	4.22E-3	1.01	1.10	1.10	1.01
17	13 474 584	80 968	7363	4.08E-3	7.44E-2	7.39E-1	4.07E-3	4.07E-3	3.87E-2	4.25E-1	4.04E-3	1.00	1.92	1.74	1.01
18	1 300 149	56 589	15 219	4.25E-3	2.73E-2	1.01E-1	4.03E-3	4.09E-3	1.45E-2	5.29E-2	3.87E-3	1.04	1.88	1.92	1.04
19	291 621 648	115 593 125	141 357	5.44E-3	9.79E-3	5.20	5.02E-3	4.17E-3	4.64E-3	1.78	3.22E-3	1.31	2.11	2.92	1.56
20	730 051	39 948	147 097	4.87E-3	2.64E-2	7.89E-3	3.94E-3	4.40E-3	1.99E-2	6.35E-3	3.57E-3	1.11	1.33	1.24	1.10
21	8 193 072	232 484	13 915	4.21E-3	3.34E-2	5.39E-1	4.10E-3	4.12E-3	1.53E-2	2.49E-1	4.00E-3	1.02	2.19	2.16	1.02
22	36 810 697	730 051	170 777	4.15E-3	4.06E-2	1.74E-1	4.05E-3	4.10E-3	2.10E-2	8.90E-2	4.01E-3	1.01	1.94	1.95	1.01
23	504 075 182	421 415 583	23 291 146	6.81E-3	7.45E-3	1.15E-1	4.04E-3	4.95E-3	5.08E-3	5.65E-2	3.22E-3	1.38	1.47	2.04	1.25
24	9 898 122	11 180	6343	4.01E-3	1.70E-1	2.99E-1	4.00E-3	4.01E-3	1.01E-1	1.78E-1	4.00E-3	1.00	1.68	1.68	1.00
25	2 287 410 615	484 406 343	4 290 994	4.89E-3	1.33E-2	1.17	4.47E-3	4.40E-3	8.49E-3	8.43E-1	3.71E-3	1.11	1.57	1.39	1.20
26	193 929 303	21 724 073	98 798	4.56E-3	1.77E-2	2.74	4.53E-3	4.15E-3	6.35E-3	1.06	3.75E-3	1.10	2.79	2.58	1.21
27	34 407	4304	464	3.22E-3	1.23E-2	1.10E-1	2.84E-3	2.97E-3	7.07E-3	6.05E-2	2.62E-3	1.08	1.73	1.83	1.08
28	6 714 588	32 737	20 511	3.98E-3	8.22E-2	1.31E-1	3.95E-3	3.97E-3	4.87E-2	7.77E-2	3.94E-3	1.00	1.69	1.69	1.00
29	640 041 725	18 343 319	38 305 359	4.37E-3	3.45E-2	1.67E-2	4.05E-3	4.21E-3	2.51E-2	1.24E-2	3.90E-3	1.04	1.38	1.34	1.04
30	421 415 583	3 059 364	1 034 193	4.06E-3	6.75E-2	1.99E-1	4.03E-3	4.04E-3	3.78E-2	1.11E-1	4.00E-3	1.01	1.78	1.79	1.01
31	6 699 655 944	2 428 132 460	465 504 975	6.59E-3	1.38E-2	6.79E-2	4.77E-3	6.26E-3	1.26E-2	6.17E-2	4.54E-3	1.05	1.09	1.10	1.05
32	374 818	56 589	136	4.33E-3	1.49E-2	4.29	4.36E-3	3.73E-3	4.31E-3	1.32	3.27E-3	1.16	3.45	3.24	1.33
33	540 436 824	847 567	11 153 450	4.10E-3	1.46E-1	1.16E-2	4.02E-3	4.07E-3	1.17E-1	9.60E-3	3.98E-3	1.01	1.25	1.21	1.01
34	647 883	2323	65 699	4.29E-3	9.89E-2	4.65E-3	3.89E-3	4.13E-3	7.78E-2	4.12E-3	3.75E-3	1.04	1.27	1.13	1.04
35	10 933 683	7 343 645	6343	6.18E-3	8.06E-3	5.84	5.11E-3	4.17E-3	4.20E-3	1.51	2.95E-3	1.48	1.92	3.85	1.73
36	377 724 782	291 621 648	1 717 874	6.35E-3	7.70E-3	9.43E-1	4.43E-3	4.94E-3	5.50E-3	6.28E-1	3.30E-3	1.29	1.40	1.50	1.34
37	640 041 725	1 131 081	2 138 265	4.11E-3	1.38E-1	7.32E-2	4.09E-3	4.10E-3	9.68E-2	5.13E-2	4.08E-3	1.00	1.43	1.43	1.00
38	216 843	206 318	36 525	6.98E-3	7.25E-3	3.45E-2	3.78E-3	4.69E-3	4.86E-3	1.83E-2	2.81E-3	1.49	1.49	1.88	1.34
39	1 237 048	232 484	778	4.78E-3	1.37E-2	2.86	4.65E-3	4.10E-3	4.76E-3	9.58E-1	3.50E-3	1.17	2.88	2.98	1.33
40	5 886 737 105	227 397 359	44 471 331	4.54E-3	3.32E-2	1.69E-1	4.35E-3	4.46E-3	2.73E-2	1.38E-1	4.27E-3	1.02	1.22	1.22	1.02

contrast, the ML method uses all the information as it incorporates each individual value of the sufficient statistic.

7 OUTLOOK

As we have shown, the ML method is able to improve the cardinality estimates for results of set operations between two HLL sketches. Unfortunately, joint cardinality estimation is much more expensive than for a single sketch, because it requires maximization of a multi-dimensional function. Since we have found the improved estimator which is almost as precise as the ML estimator for the single sketch case, we could imagine that there also exists a faster algorithm for joint cardinality estimation of two sketches. It is expected that such a new algorithm makes use of all the information given by the sufficient statistic (19).

The ML method can also be used to estimate distance measures such as the Jaccard distance of two sets that are represented as HLL sketches. This directly leads to the question whether the HLL algorithm could be used for locality-sensitive hashing [16, 25]. The HLL algorithm itself can be regarded as hashing algorithm as it maps sets to register values. For sufficiently large cardinalities we can use the Poisson approximation and assume that the number of zero-valued HLL registers can be ignored. Furthermore, if $p + q$

is chosen large enough, the number of saturated registers can be ignored as well. As a consequence, we can simplify (17) and assume that K_1 and K_2 are distributed according to

$$P(K_1 \leq k_1 \wedge K_2 \leq k_2) = e^{-\frac{\lambda_a}{m_2^{k_1}} - \frac{\lambda_b}{m_2^{k_2}} - \frac{\lambda_x}{m_2^{\min(k_1, k_2)}}}$$

which yields

$$P(K_1 = K_2) = \sum_{k=-\infty}^{\infty} P(K_1 = k \wedge K_2 = k) = \sum_{k=-\infty}^{\infty} e^{-\frac{\lambda_a + \lambda_b + \lambda_x}{m_2^k}} \left(1 - e^{-\frac{\lambda_a + \lambda_x}{m_2^k}} - e^{-\frac{\lambda_b + \lambda_x}{m_2^k}} + e^{-\frac{\lambda_a + \lambda_b + \lambda_x}{m_2^k}} \right).$$

for the probability that a register has the same value in both sketches. Using the approximation $\sum_{k=-\infty}^{\infty} e^{-\frac{x}{2^k}} - e^{-\frac{y}{2^k}} \approx 2\alpha_\infty(\log(y) - \log(x))$, which is obtained by integrating $\xi(x) \approx 1$ on both sides, we get

$$P(K_1 = K_2) \approx 1 + 2\alpha_\infty \log \left(1 - \frac{1}{2}D + \frac{1}{4}D^2 \frac{\lambda_a \lambda_b}{(\lambda_a + \lambda_b)^2} \right) \quad (20)$$

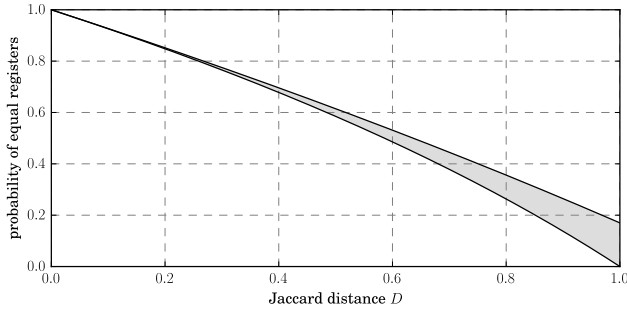


Figure 10: The approximate probability range of equal register values as a function of the Jaccard distance.

where $D = \frac{\lambda_a + \lambda_b}{\lambda_a + \lambda_b + \lambda_x}$ corresponds to the Jaccard distance. Since $\frac{\lambda_a \lambda_b}{(\lambda_a + \lambda_b)^2}$ is always in the range $[0, \frac{1}{4}]$, the probability for equal register values can be bounded by $1 + 2\alpha_\infty \log(1 - \frac{1}{2}D) \leq P(K_1 = K_2) \leq 1 + 2\alpha_\infty \log(1 - \frac{1}{2}D + \frac{1}{16}D^2)$ as shown in Fig. 10. This dependency on the Jaccard distance makes the HLL algorithm an interesting candidate for locality-sensitive hashing. Furthermore, the method described in Section 6 would allow a more detailed estimation of the Jaccard distance by using the estimates for intersection and union sizes. This could be used for additional more precise filtering when searching for similar items. Since HLL sketches can be efficiently constructed, because only a single hash function evaluation is needed for each item, the preprocessing step would be very fast. In contrast, preprocessing is very costly for minwise hashing, because of the many required permutations [17].

8 CONCLUSION

Based on the Poisson approximation we have presented two new methods to estimate the number of distinct elements from HLL sketches. Unlike previous approaches that use patchworks of different estimators or rely on empirically determined data, the presented ones are inherently unbiased over the full cardinality range. The first extends the original estimator by theoretically derived correction terms in order to obtain an improved estimator that can be straightforwardly translated into a fast algorithm. Due to its simplicity we believe that it has the potential to become the standard textbook cardinality estimator for HLL sketches. The second estimation approach is based on the ML method and can also be applied to two sketches which significantly improves cardinality estimates for corresponding intersections, relative complements, and unions compared to the conventional approach using the inclusion-exclusion principle.

REFERENCES

- [1] N. Alon, Y. Matias, and M. Szegedy. 1999. The Space Complexity of Approximating the Frequency Moments. *J. Comput. System Sci.* 58, 1 (1999), 137–147.
- [2] K. Beyer, P. J. Haas, B. Reinwald, Y. Sismanis, and R. Gemulla. 2007. On Synopses for Distinct-Value Estimation Under Multiset Operations. In *Proc. of the 26th ACM SIGMOD International Conference on Management of Data*. Beijing, China, 199–210.
- [3] G. Casella and R. L. Berger. 2002. *Statistical Inference* (2nd ed.). Duxbury, Pacific Grove, CA, USA.
- [4] A. Chen, J. Cao, L. Shepp, and T. Nguyen. 2011. Distinct Counting with a Self-Learning Bitmap. *J. Am. Stat. Assoc.* 106, 495 (2011), 879–890.
- [5] E. Cohen. 2015. All-Distances Sketches, Revisited: HIP Estimators for Massive Graphs Analysis. *IEEE Transactions on Knowledge and Data Engineering* 27, 9 (2015), 2320–2334.
- [6] E. Cohen and H. Kaplan. 2007. Summarizing Data Using Bottom-k Sketches. In *Proc. of the 26th Annual ACM Symposium on Principles of Distributed Computing*. New York, NY, USA, 225–234.
- [7] R. Cohen, L. Katzir, and A. Yehezkel. 2016. A Minimal Variance Estimator for the Cardinality of Big Data Set Intersection. (2016). arXiv:1606.00996
- [8] A. Dasgupta, K. Lang, L. Rhodes, and J. Thaler. 2015. A Framework for Estimating Stream Expression Cardinalities. (2015). arXiv:1510.01455
- [9] M. Durand and P. Flajolet. 2003. Loglog Counting of Large Cardinalities. In *Proc. of the 11th Annual European Symposium on Algorithms*. Budapest, Hungary, 605–617.
- [10] O. Ertl. 2017. New cardinality estimation algorithms for HyperLogLog sketches. (2017). arXiv:1702.01284
- [11] P. Flajolet, É. Fusy, O. Gandouet, and F. Meunier. 2007. Hyperloglog: The Analysis of a Near-Optimal Cardinality Estimation Algorithm. In *Proc. of the 13th Conference on Analysis of Algorithms*. Juan des Pins, France, 127–146.
- [12] S. Heule, M. Nunkesser, and A. Hall. 2013. Hyperloglog in Practice: Algorithmic Engineering of a State of the Art Cardinality Estimation Algorithm. In *Proc. of the 16th International Conference on Extending Database Technology*. Genoa, Italy, 683–692.
- [13] P. Indyk and D. Woodruff. 2003. Tight Lower Bounds for the Distinct Elements Problem. In *Proc. of the 44th Annual IEEE Symposium on Foundations of Computer Science*. Cambridge, MA, USA, 283–288.
- [14] D. M. Kane, J. Nelson, and D. P. Woodruff. 2010. An Optimal Algorithm for the Distinct Elements Problem. In *Proc. of the 29th ACM SIGMOD-SIGACT-SIGART Symposium on Principles of Database Systems*. Indianapolis, IN, USA, 41–52.
- [15] D. E. King. 2009. Dlib-ml: A Machine Learning Toolkit. *Journal of Machine Learning Research* 10 (2009), 1755–1758.
- [16] J. Leskovec, A. Rajaraman, and J. D. Ullman. 2014. *Mining of Massive Datasets* (2nd ed.). Cambridge University Press.
- [17] P. Li and A. C. König. 2011. Theory and Applications of b-bit Minwise Hashing. *Commun. ACM* 54, 8 (2011), 101–109.
- [18] A. Metwally, D. Agrawal, and A. E. Abbadi. 2008. Why Go Logarithmic If We Can Go Linear?: Towards Effective Distinct Counting of Search Traffic. In *Proc. of the 11th International Conference on Extending Database Technology*. Nantes, France, 618–629.
- [19] A. Pascoe. 2013. HyperLogLog and MinHash - A Union for Intersections. <http://tech.adroll.com/media/hllminhash.pdf>. (2013).
- [20] W. H. Press. 2007. *Numerical Recipes: The Art of Scientific Computing* (3rd ed.). Cambridge University Press.
- [21] L. Rhodes. 2015. System and Method for Enhanced Accuracy Cardinality Estimation. (Sept. 24 2015). US Patent 20,150,269,178.
- [22] S. Sanfilippo. 2014. Redis New Data Structure: The HyperLogLog. <http://antirez.com/news/75>. (2014).
- [23] D. Ting. 2014. Streamed Approximate Counting of Distinct Elements: Beating Optimal Batch Methods. In *Proc. of the 20th ACM SIGKDD International Conference on Knowledge Discovery and Data Mining*. New York, NY, USA, 442–451.
- [24] D. Ting. 2016. Towards Optimal Cardinality Estimation of Unions and Intersections with Sketches. In *Proc. of the 22nd ACM SIGKDD International Conference on Knowledge Discovery and Data Mining*. San Francisco, CA, USA, 1195–1204.
- [25] J. Wang, H. T. Shen, J. Song, and J. Ji. 2014. Hashing for Similarity Search: A Survey. (2014). arXiv:1408.2927
- [26] K.-Y. Whang, B. T. Vander-Zanden, and H. M. Taylor. 1990. A Linear-Time Probabilistic Counting Algorithm for Database Applications. *ACM Transactions on Database Systems* 15, 2 (1990), 208–229.